

PARAMETRIC TESTS OF A 40 A h BIPOLAR NICKEL-HYDROGEN BATTERY

ROBERT L CATALDO

National Aeronautics and Space Administration, Lewis Research Center, Cleveland, OH 44135 (U S A)

Summary

A series of tests was performed to characterize battery performance relating to certain operating parameters which included charge current, discharge current, temperature, and pressure. The parameters were varied to confirm battery design concepts and to determine optimal operating conditions.

Introduction

Spacecraft power requirements are constantly increasing. Special spacecraft such as the Space Station and platforms will require energy storage systems of 130 kilowatt hours and 25 kilowatt hours, respectively. The complexity of these high power systems will demand high reliability, and reduced mass and volume. Candidate electrochemical systems are regenerative fuel cells, nickel-cadmium batteries and nickel-hydrogen batteries.

A system that uses batteries for storage will require a cell count in excess of 400 units. These cell units must then be assembled into several batteries with over 100 cells in a series connected string. In an attempt to simplify the construction of conventional cells and batteries, the NASA Lewis Research Center battery systems group initiated work on a nickel-hydrogen battery, in a bipolar configuration, in early 1981.

Features of the battery with this bipolar construction show promise in improving both volumetric and gravimetric energy densities as well as thermal management. Bipolar construction allows cooling in closer proximity to the cell components, thus heat removal can be accomplished at a higher rejection temperature than conventional cell designs. Also, higher discharge current densities are achievable because of low cell impedance. Lower cell impedance is achieved via current flow perpendicular to the electrode face, thus reducing voltage drops in the electrode grid and electrode terminal tabs.

Battery and cell design

The battery tested was a 12 V (10 cell), 40 A h, bipolar battery. The battery was actively cooled with five inter-cell planar cooling plates. The cooling system was operated in the temperature range 0 - 40 °C, allowing full thermal characterization and determination of appropriate operating temperature.

Accommodations were made for oxygen and electrolyte management. These two functions take place within an electrolyte reservoir plate that contains the oxygen recombination sites. Water, the product of recombination, equilibrates with the electrolyte of the nickel electrode. These functions and other design details are explained in greater depth in a previous paper [1].

Test procedures

Two initialization cycles were performed prior to characterization. The cycle regime was a $C/10$ (5.0 A), 13 h charge and a $C/4$ (12 A) discharge terminated when the first cell reached 0.5 V. A value of 50 A h was used for the capacity, C , which had been determined from previous test results. The ampere hours obtained on discharge during the first cycle was 49, and 50 on the second cycle. The results showed that this new battery design could provide the predicted results.

Battery performance was characterized by carrying out a series of parametric tests. Data were obtained at the following conditions: charge rates of C and $C/2$, discharge rates of $2C$, C and $C/4$, temperatures of 0, 10, 20, 30 and 40 °C, base pressures of 200 and 400 pounds per square inch.

Temperatures were maintained by circulating a non-conductive, inert fluid through the five cooling plates of the battery. Temperatures were adjusted at static conditions and allowed to stabilize until the inlet and outlet coolant temperatures were equal. The coolant bath temperature was maintained to within 0.1 °C by the chiller/heater unit.

The hydrogen pressure was also adjusted in the discharged condition. The amount of hydrogen generated on charge was small compared with the free volume of the test chamber. Thus, the pressure increase from discharged to full charge was only about 25 lb in.⁻²

Test results

Data taken for each charge/discharge cycle were as follows: individual cell voltages, temperatures, ampere hours and watt hours. Values were updated and integrated every 18 s with a digitizing voltmeter. Both charge and discharge current levels were held constant with power supplies and electronic discharge devices.

Tables 1 and 2 show the test results in ampere hours, watt hours and end-of-discharge battery voltage. The remaining battery capacity was drained at the 12 A rate ($C/4$) when the discharge rate was greater than $C/4$. Charge input was 56 A h for each test matrix point. The data presented in Table 2, 400 psi gas pressure, were a modified matrix where the effects of hydrogen gas pressure could be observed at only those conditions of greatest interest. Table 3 shows characterization data obtained at all pressure and temperature levels at the same charge rate of 2 h and the same 50 A (the C rate) discharge. The decision was made to increase the charge input to 65 A h for this series of tests for two reasons.

(i) because the $C/4$ drain resulted in total discharge capacities of 54 A h several times, thereby creating a situation of possible charge deficiency;

(ii) to minimize the influence of varying levels of charge acceptance of the nickel electrode at different temperatures.

TABLE 1

Test matrix data at 200 psi

Charge rate	Discharge rate	Temp (°C)	Ampere hours out	Watt hours		Energy efficiency	End of discharge battery voltage
				in	out		
C	$2C$	0	42.4	879	468	53	9.3
C	C	0	44.4	882	533	60	10.4
C	$C/4$	0	49.3	883	629	71	10.8
$C/2$	$2C$	0	43.8	845	469	55	8.8
$C/2$	C	0	46	845	545	64	10.2
$C/2$	$C/4$	0	51.5	851	655	77	10.4
C	$2C$	10	43.6	856	497	58	9.5
C	C	10	46	860	557	65	9.8
C	$C/4$	10	51	856	648	75	10.1
$C/2$	$2C$	10	43.5	831	489	59	9.3
$C/2$	C	10	45	834	539	65	9.9
$C/2$	$C/4$	10	52	840	656	78	9.9
C	$2C$	20	45.5	843	529	63	9.5
C	C	20	47.5	842	582	69	10.1
C	$C/4$	20	51.5	818	652	80	8.4
$C/2$	$2C$	20	45	822	524	64	9.5
$C/2$	C	20	48	820	587	72	9.7
$C/2$	$C/4$	20	51.5	820	655	80	9.6
C	$2C$	30	43	834	505	60	10.1
C	C	30	46	834	560	67	10.5
C	$C/4$	30	50	832	639	77	9.5
$C/2$	$2C$	30	40	818	470	57	10.5
$C/2$	C	30	44	813	536	66	10.4
$C/2$	$C/4$	30	49	818	629	77	9.7
C	C	40	41.8	824	520	63	10.6
$C/2$	C	40	41.5	809	516	64	10.5

TABLE 2

Test matrix data at 400 psi

Charge rate	Discharge rate	Temp (°C)	Ampere hours out	Watt hours		Energy efficiency	End of discharge battery voltage
				in	out		
<i>C</i>	<i>C</i>	0	37	890	452	51	10.9
<i>C/2</i>	<i>C</i>	0	39	857	470	55	10.7
<i>C</i>	<i>C</i>	10	37.8	870	466	53.5	11.0
<i>C/2</i>	<i>C</i>	10	38.5	841	474	56	10.8
<i>C</i>	<i>C</i>	20	39.4	851	490	57	11.0
<i>C/2</i>	<i>C</i>	20	39.6	829	495	60	10.8
<i>C</i>	<i>C</i>	30	42.2	836	523	62.5	9.3
<i>C/2</i>	<i>C</i>	30	42.2	824	523	63.5	9.1
<i>C</i>	<i>C</i>	40	45.5	827	569	69	8.7
<i>C/2</i>	<i>C</i>	40	41.8	816	521	64	8.9

TABLE 3

Characterization test matrix data (2 h 32.5 A charge, *C* rate (50 A) discharge)

Temp (°C)	Pressure (base)	Ampere hours out	Watt hours		Wh efficiency	End of discharge voltage
			in	out		
0	400	44	1015	514	51	9.7
10	400	44	1000	524	52	9.9
20	400	46	978	554	56.5	9.0
30	400	48	967	575	60	8.9
40	400	45	980	553	56.5	8.9
0	200	43	1018	502	49	9.7
10	200	42	1007	502	50	10
20	200	42	975	506	52	10.3
30	200	44	970	532	55	9.8
40	200	42	957	510	53	8.6

Special tests were also conducted to determine battery performance beyond the normally expected range of conventional space power systems. High discharge rates and pulse discharge capabilities were tested because the bipolar battery has exhibited good performance in this area, as previously reported [2].

The battery was high-rate discharged at both constant and pulsed currents for the 250 A (5 *C*) and 500 A (10 *C*) rates to a discharge cutoff voltage of 6.0 V during the pulse. One additional pulse test was to discharge the battery at 1500 A (30 *C*) for 1 s where a load voltage of 4.0 V was established resulting in a 6 kW pulse. This value was lower than expected

from previous results [2]. This lower value of pulse power, and the resulting dramatic increase in high rate capacity by pulsing compared with constant discharge level, indicated that possibly the area for hydrogen gas access in the frames was not sufficient to support these high discharge rates. This problem was addressed by redesigning the gas access slots in future batteries for pulse applications

Figure 1 shows plots of the data tabulated in Table 1 and results of the special pulse tests. Figure 1 displays battery voltage and discharge capacity as a function of discharge current at 20 °C. The 12, 50 and 100 A discharge plots are characteristic of classical battery performance plots. The constant load discharge curves of 250 and 500 A, however, do not have the standard plateau and knee. This is because of the high rate discharge and possibly the decrease of hydrogen gas concentration at the electrode surface. These two tests were repeated by pulse discharging at a one-second-on, one-second-off duty-cycle. The "off", or relaxation time allows the gas concentration to increase in the gas cavity formed by the hydrogen electrode, gas screen, and bipolar plate. The dashed curve in Fig. 1 shows the increase in capacity discharged and the increase in watts and watt hours. The greatest change is noticed at the 250 A level where the hydrogen gas concentration depletion is less than that at the 500 A rate. An increase in ratio of off- to on-time may have improved the pulse performance, particularly at higher rates.

Figure 2 shows the relationship of energy delivered on discharge to battery temperature. The cooling configuration dictates that nickel electrode temperatures were equal over its entire area. A marked increase in energy delivered and cyclic efficiency was observed at the 30 °C data point compared

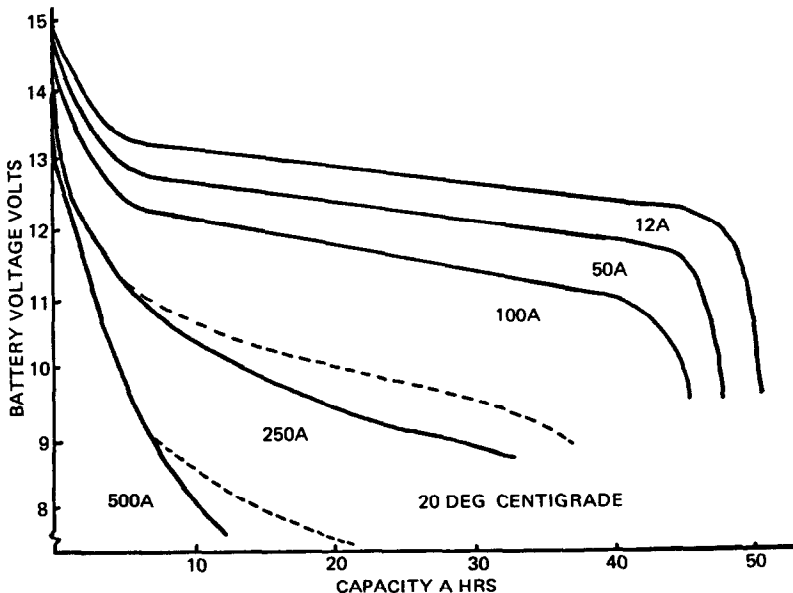


Fig 1 Plots of data contained in Table 1 Battery voltage and discharge capacity as a function of discharge current at 20 °C

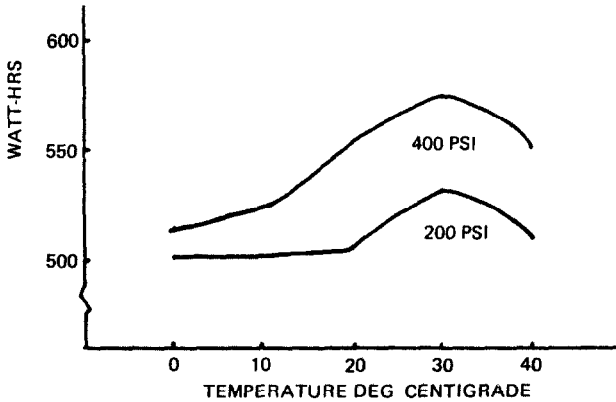


Fig 2 Relationship of energy delivered on discharge (W h) to battery temperature ($^{\circ}\text{C}$)

with both higher and lower temperatures. At temperatures lower than 30°C , battery voltage increases on charge and decreases on discharge causing a net decrease in efficiency. Above 30°C , however, the effects of nickel electrode charging efficiency were seen. These results indicate that a bipolar battery with intercell, planar cooling plates could operate at a higher system temperature than conventional single cell designs that transmit heat in a radial direction via the vessel wall. Therefore, thermal system designs would need to consider the differences in battery design.

Figure 3 shows the battery voltage profile response to pulse discharges of 500 A. Only the first four cycles are shown here, although 155 pulses (21.5 A h) were discharged. The battery voltage drop during the pulse increased from 1.4 V to 2.2 V from beginning to end. This increase in voltage drop indicates that a 30% change in effective internal cell impedance occurred.

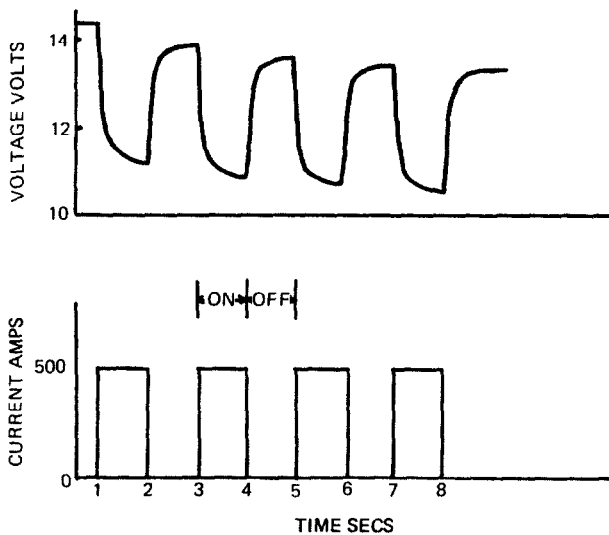


Fig 3 Battery voltage profile response to pulse discharges of 500 A

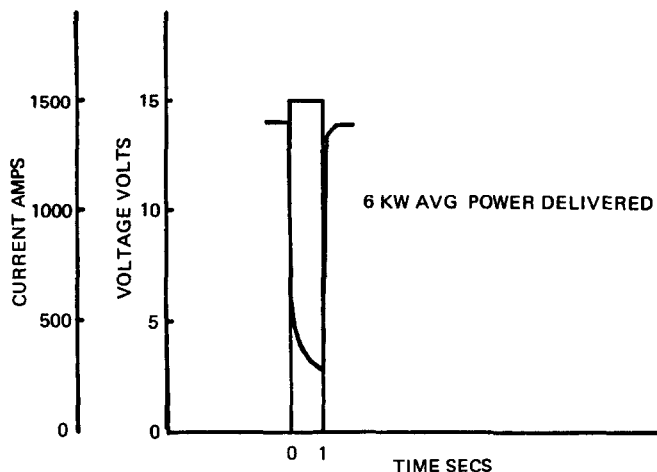


Fig 4 Voltage profile for a one pulse (1500 A, 1 s) maximum power test

Figure 4 shows the voltage profile for a one pulse maximum power test. A 1500 A 1 s pulse was delivered. Battery voltage, measured at the external terminals of the vessel, was 4.0 V, resulting in a power level of 6 kW. The instantaneous voltage drop was 8 V for the 1500 A pulse. Using these values, a cell resistance of about 0.5 m Ω was calculated.

Conclusions

The parametric tests conducted on the first actively cooled bipolar nickel-hydrogen battery demonstrate its feasibility. The results are comparable with previous NASA/Lewis designs except for its high rate performance. The pulse tests conducted suggest an insufficient gas access to the hydrogen electrode which has resulted in increased polarization. This area has been addressed in other designs for high discharge rates.

The thermal aspects of this battery allow cooling system temperatures of about 30 °C for maximum power efficiency. Battery operation in this temperature range of 30 °C could have an impact on solar array and radiator sizing.

The NASA/Lewis Research Center is working toward establishing a baseline design that would require only simple, low cost modifications to the baseline design for integration into various applications. The successful application of active cooling is a major step in developing this baseline design.

References

- 1 R L Cataldo, Design of a 1 kW h bipolar nickel-hydrogen battery, *NASA memorandum*, 1984
- 2 R L Cataldo, Test results of a ten cell bipolar nickel-hydrogen battery, *NASA memorandum*, 1983